

Mechanism of Cooperative Catalysis in a Lewis Acid Promoted Nickel-Catalyzed Dual C–H Activation Reaction

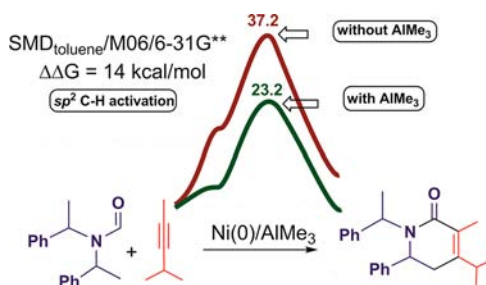
Megha Anand and Raghavan B. Sunoj*

Department of Chemistry, Indian Institute of Technology Bombay, Powai,
Mumbai 400076, India

sunoj@chem.iitb.ac.in

Received July 24, 2012

ABSTRACT



The mechanism of cooperativity offered by AlMe_3 in a Ni-catalyzed dehydrogenative cycloaddition between substituted formamides and an alkyne is investigated by using DFT(SMD_{toluene}/M06/6-31G**) methods. The preferred pathway is identified to involve dual C–H activation, with first a higher barrier formyl C(sp^2)–H oxidative insertion followed by benzylic methyl C(sp^3)–H activation. The cooperativity is traced to be of kinetic origin as evidenced by stabilized transition states when AlMe_3 is bound to the formyl group, particularly in the oxidative insertion step.

Applications and methodological developments in the domain of C–H activation reactions remained in the forefront of catalysis over the past couple of decades.¹ While the quest for newer catalysts for selective C–H functionalizations continues to remain prevalent in contemporary literature, novel strategies making use of cooperative catalysis are now receiving increasing attention.² The concept of cooperativity as invoked toward appreciating the underpinning of enzymatic processes in Nature can

be regarded as a key source of inspiration to chemists.³ In recent times, different types of catalysts are orchestrated to work in a cooperative fashion to produce improved and expedient synthetic protocols.⁴ In cooperative catalysis, the complementary attributes of multiple catalysts are made to work in tandem. The combinations that received considerable recent attention include metal–metal, metal–organo, and organo–organo cooperative catalysis.⁵

In a series of recent activities in cooperative approaches in transition metal catalysis, the Hiyama group employed

(1) (a) Crabtree, R. H. *Chem. Rev.* **1985**, *85*, 245. (b) Labinger, J. A.; Bercaw, J. E. *Nature* **2002**, *417*, 507. (c) Godula, K.; Sames, D. *Science* **2006**, *312*, 67 and references therein. (d) Dick, A. R.; Sanford, M. S. *Tetrahedron* **2006**, *62*, 2439. (e) Bergman, R. G. *Nature* **2007**, *446*, 391. (f) Gunay, A.; Theopold, K. H. *Chem. Rev.* **2010**, *110*, 1060. (g) Mkhaliid, I. A. I.; Barnard, J. H.; Marder, T. B.; Murphy, J. M.; Hartwig, J. F. *Chem. Rev.* **2010**, *110*, 890. (h) Doyle, M. P.; Duffy, R.; Ratnikov, M.; Zhou, L. *Chem. Rev.* **2010**, *110*, 704. (i) Balcells, D.; Clot, E.; Eisenstein, O. *Chem. Rev.* **2010**, *110*, 749.

(2) (a) Kumagai, N.; Shibasaki, M. *Angew. Chem., Int. Ed.* **2011**, *50*, 4760. (b) North, M. *Angew. Chem., Int. Ed.* **2010**, *49*, 8079. (c) Knowles, R. R.; Jacobsen, E. R. *Proc. Natl. Acad. Sci. U.S.A.* **2010**, *107*, 20678. (d) Xu, H.; Zuend, S. J.; Woll, M. G.; Tao, Y.; Jacobsen, E. N. *Science* **2010**, *327*, 986. (e) Zhao, X.; DiRocco, D. A.; Rovis, T. *J. Am. Chem. Soc.* **2011**, *133*, 12466.

(3) Hammes, G. G.; Benkovic, S. J.; Hammes-Schiffer, S. *Biochemistry* **2011**, *50*, 10422.

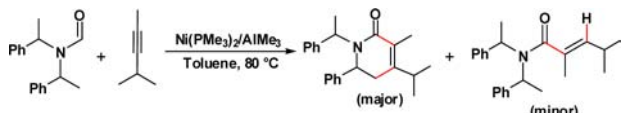
(4) Rueping, M. *Angew. Chem., Int. Ed.* **2010**, *16*, 9350. (b) (a) Paull, D. H.; Abraham, C. J.; Scerba, M. T.; Alden-Danforth, E.; Lectka, T. *Acc. Chem. Res.* **2008**, *41*, 655. (c) Duschek, A.; Kirsch, S. F. *Angew. Chem., Int. Ed.* **2008**, *47*, 5703. (d) Zhang, Z.; Wang, Z.; Zhang, R.; Ding, K. *Angew. Chem., Int. Ed.* **2010**, *49*, 6746. (e) Burns, N. Z.; Witten, M. R.; Jacobsen, E. N. *J. Am. Chem. Soc.* **2011**, *133*, 14578. (f) Armas, P. D.; Tejedor, D.; Garcia-Tellado, F. *Angew. Chem., Int. Ed.* **2010**, *49*, 1013. (g) Mo, J.; Chen, X.; Chi, Y. R. *J. Am. Chem. Soc.* **2012**, *134*, 8810.

(5) (a) Park, Y. J.; Park, J.-W.; Jun, C.-H. *Acc. Chem. Res.* **2008**, *41*, 222. (b) Yeung, C. S.; Dong, V. M. *Angew. Chem., Int. Ed.* **2011**, *50*, 809. (c) Quintard, A.; Alexakis, A.; Mazet, C. *Angew. Chem., Int. Ed.* **2011**, *50*, 2354. (d) Nakao, Y.; Yada, A.; Hiyama, T. *J. Am. Chem. Soc.* **2010**, *132*, 10024. (e) Li, C.; Villa-Marcos, B.; Xiao, J. *Am. Chem. Soc.* **2009**, *131*, 6967. (f) Ogoshi, S.; Ueta, M.; Arai, T.; Kurosawa, H. *J. Am. Chem. Soc.* **2005**, *127*, 12810.

substrate activation by using Lewis acids.⁶ In a more recent development, an interesting cooperative dual C–H activation using Ni(0)/trialkyl aluminum was demonstrated as capable of producing an array of synthetically useful cyclic compounds.⁷

While experimental advances in cooperative catalysis are currently witnessing an impressive stride, the mechanistic understanding of such reactions remains generally inadequate. In particular, the molecular and energetic origin of cooperativity is not yet well established. Quantitative assessment of the role of Lewis acids in a complex catalytic reaction, particularly in key steps such as oxidative insertion and reductive elimination, is not widely reported. As part of our continued interest toward the mechanism of catalytic reactions, we have examined the title reaction (Scheme 1) involving dual C–H activation, with the objective of unraveling the mechanism and the role of Lewis acids.

Scheme 1. Dehydrogenative Cycloaddition between Formamide and Alkyne Leading to Dihydropyridinone (ref 7)

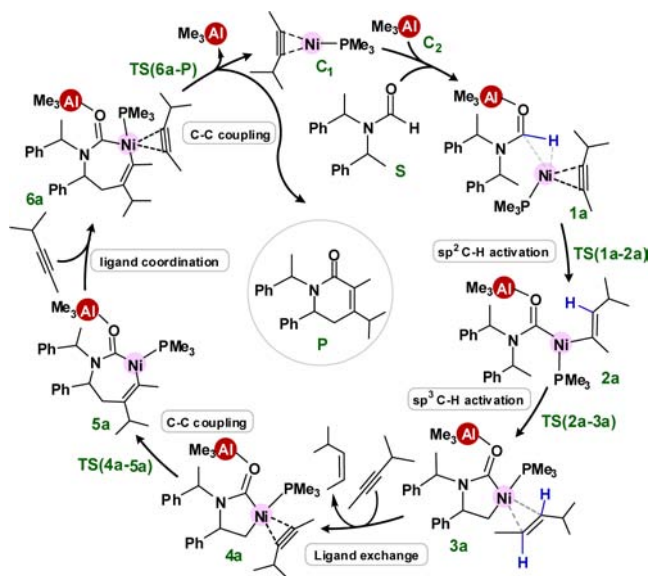


Two key mechanistic scenarios, with and without the direct involvement of AlMe₃, are examined by using Gibbs free energies computed at the SMD_{toluene}/M06/6-31G**//M06/6-31G** level of theory.⁸ The dehydrogenative cycloaddition with alkynes is achieved by the activation of formyl and alkyl C–H bonds respectively of formamide and the methyl group of benzyl moieties. While a preference for C(sp²)–H over C(sp³)–H activation is generally known, some examples suggest that this can even be competitive.⁹ The preferred order of this dual C–H activation leading to cyclic dihydropyridinone as the major product is therefore investigated, and the controlling factors are delineated.

The catalytic cycle can be envisaged to begin with a Ni(0)–alkyne complex (C₁) as shown in Scheme 2. The formation of a catalyst–substrate complex between C₁ and the AlMe₃-bound substrate (*R,R*)-N,N-bis(1-phenylethyl)formamide is the first key step. The electron-rich Ni(0) can interact with either the formyl C–H or the methyl

C–H bonds. Depending on the order of activation of the C–H bonds, two mechanistic pathways are herein proposed. In pathway 1, formyl C–H is activated by selective interaction of nickel with the C(sp²)–H bond as in **1a**, while, in pathway 2, the benzylic methyl group is activated (**1a'**).

Scheme 2. Mechanism of Ni/AlMe₃ Cooperative Catalysis Involving Dual C–H Activation Beginning with Formyl C(sp²)–H Activation (pathway 1)



First, the details of pathway 1 are presented. Oxidative insertion of nickel into the C(sp²)–H bond leads to a Ni(II) intermediate **2a**. Improved proximity between the benzylic methyl and the nickel center in **2a** would facilitate the activation of the C(sp³)–H bond via transition state **TS(2a-3a)** to provide a five-membered nickelacycle intermediate **3a**.¹⁰ The process involves the transfer of hydrogen from the benzylic methyl group to the alkenyl carbon bound to nickel. In line with the commonly proposed dissociative mechanism, the displacement of an alkenyl side product from the metal by a new molecule of alkyne resulting in an alkyne bound nickelacycle **4a** is considered next.¹¹ The subsequent vital step is a migratory insertion involving **TS(4a-5a)** leading to an expanded seven-membered nickelacycle **5a**. In the next step, uptake of another molecule of alkyne leads to **6a** wherein crowding around Ni(II) is relatively higher as compared to other intermediates.¹² Lastly, reductive elimination in **6a** furnishes a dihydropyridinone product (**P**) and results in the release of catalytic species C₁ so as to continue the catalytic cycle.

(6) (a) Nakao, Y.; Idei, H.; Kanyiva, S.; Hiyama, T. *J. Am. Chem. Soc.* **2009**, *131*, 5070. (b) Nakao, Y.; Yada, A.; Ebata, S.; Hiyama, T. *J. Am. Chem. Soc.* **2007**, *129*, 2428. (c) Nakao, Y.; Ebata, S.; Yada, A.; Hiyama, T.; Ikawa, M.; Ogoshi, S. *J. Am. Chem. Soc.* **2008**, *130*, 12874. (d) Nakao, Y.; Kanyiva, K. S.; Hiyama, T. *J. Am. Chem. Soc.* **2008**, *130*, 2448.

(7) (a) Nakao, Y.; Morita, E.; Idei, H.; Hiyama, T. *J. Am. Chem. Soc.* **2011**, *133*, 3264. (b) In real system, the phosphine ligand is P^tBu₃.

(8) (a) Full details of computational methods are provided in the Supporting Information. (b) All calculations were done using the Gaussian09 suite of programs (Rev. A.02). Frisch, M. J. et al. Gaussian Inc., Wallingford, CT. See Supporting Information for full reference.

(9) (a) Goldman, A. S.; Goldberg, K. I. In *Activation and Functionalization of C–H Bonds*; Goldman, A. S., Goldberg, K. I., Eds.; ACS Symposium Series 885; American Chemical Society: Washington, DC, 2004. (b) Crosby, S. H.; Clarkson, G. J.; Rourke, J. P. *J. Am. Chem. Soc.* **2009**, *131*, 14142.

(10) A number of interesting experimental reports on nickelacycles are known. (a) Ceder, R. M.; Muller, G.; Ordinas, M.; Maestro, M. A.; Bardia, M. F.; Solans, X. *J. Chem. Soc., Dalton Trans.* **2001**, 977. (b) Brown, J. S.; Sharp, P. R. *Organometallics* **2003**, *22*, 3604. (c) Cámpora, J.; Gutiérrez, E.; Monge, A.; Palma, P.; Poveda, M. L.; Ruíz, C.; Carmona, E. *Organometallics* **1994**, *13*, 1728.

(11) The energy for the formation of the side product *cis* alkene in pathway 1, as noted in the experimental report, is found to be very close to that leading to *trans* alkene through **TS(2a-3a)**. The TS for *cis* alkene formation could be located only in pathway 1. To maintain conformity between pathways 1 and 2, the *trans* isomer is shown in the schemes.

The computed Gibbs free energies are provided in the form of a reaction profile diagram in Figure 1.¹³ Two of the most preferred routes, with and without AlMe₃, are indicated to enable a direct comparison as well as to convey the key insights. The intermediates and transition states are found to be more stable in the cooperative pathway wherein the Lewis acid AlMe₃ is coordinated to the substrate. It is of high significance to note that the maximum lowering of the transition state energy (of the order of 14 kcal/mol) due to AlMe₃ coordination is predicted for the first oxidative insertion step. Equally important is to reckon that the conversion of **1a** to **2a** (or **1** to **2**, in the absence of AlMe₃) is likely to be the rate-limiting step of the reaction. The transition states for various other steps in the cooperative pathway are in general found to be ~12 kcal/mol lower as compared to that in the absence of AlMe₃ coordination. Such stabilizations are in line with the experimental observation that the reaction failed to yield products in the absence of Lewis acid. The computed Gibbs free energies in the absence of AlMe₃ coordination, indicated using pink colored stationary points in the profile, convey the involvement of higher energy transition states, such as TS(**1**–**2**), which will practically be difficult to surmount. These predictions evidently point to the cooperative action of Ni(0) in tandem with AlMe₃ in dehydrogenative cycloaddition between alkynes and substituted formamides. More importantly, the cooperativity in the present system appears to have a kinetic origin.

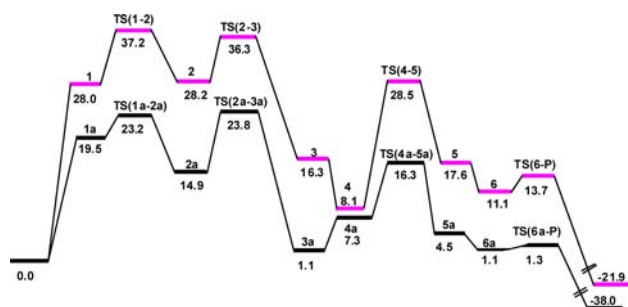


Figure 1. Gibbs free energy profile (in kcal/mol) for dehydrogenative cycloaddition catalyzed by Ni/AlMe₃ cooperative catalysis (Pathway 1). Horizontal black colored lines are for substrate bound to AlMe₃, while pink colored ones are in the absence of Lewis acid.

The optimized transition state geometries of the most important steps in the catalytic cycle with AlMe₃ are provided in Figure 2. The geometries of the corresponding

(12) Enhanced crowding at the metal center is known to ease reductive elimination. See: Alvaro, E.; Hartwig, J. F. *J. Am. Chem. Soc.* **2009**, *131*, 7858. Mann, G.; Shelby, Q.; Roy, A. H.; Hartwig, J. F. *Organometallics* **2003**, *22*, 2775. (b) However, in the present case a direct reductive elimination (TS(**5a**-P)) is found to be ~1 kcal/mol lower than through TS(**6a**-P) energy.

(13) Relative energies are computed with respect to the separated reactants Ni(COD)₂, PMe₃, formamide, and alkyne.

transition states in the absence of AlMe₃ are found to be generally similar.¹⁴ It can be noticed that in formyl C–H bond activation and the oxidative insertion step, via TS-(**1a**-**2a**), the hydrogen from the formyl carbon is transferred to the alkynic carbon through the nickel center.¹⁵ A similar metal-assisted hydrogen transfer is also noticed in the activation of the benzylic methyl C(sp³)–H bond as shown in TS(**2a**-**3a**). As with other major steps, the ring expansion of five-membered nickelacycle (**4a**) through migratory insertion transition state TS(**4a**-**5a**) to a seven-membered analogue (**5a**) conveys that the disposition of AlMe₃ generally remains away from the site of reaction. This geometric feature suggests that the lowering of transition state energies as a result of AlMe₃ coordination should have an electronic origin.

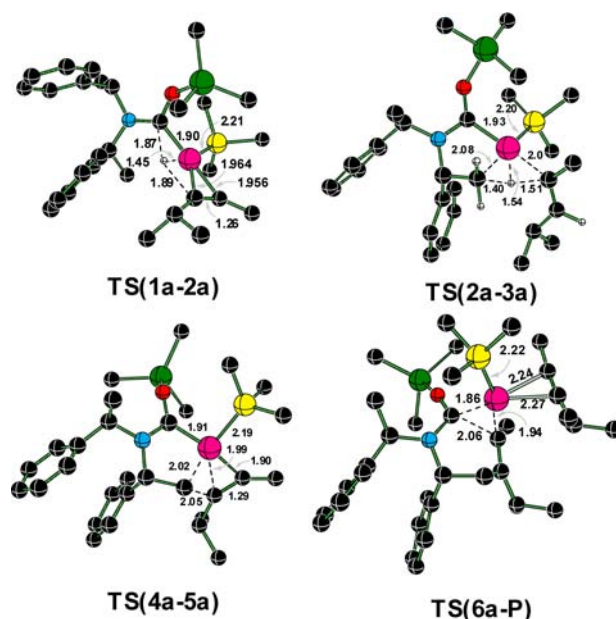


Figure 2. Optimized geometries of important transition states involved in pathway 1. Distances are in Å. Only select hydrogens are shown. Atom colors: C, black; H, ivory; O, red; N, cyan; P, yellow; Al, green; Ni, pink.

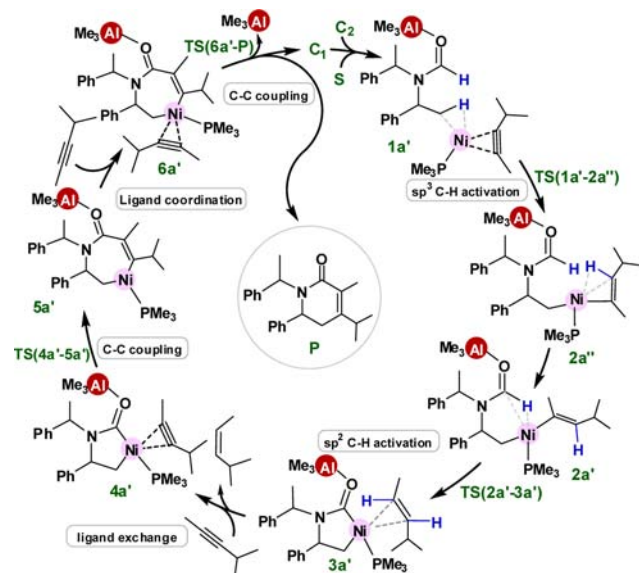
In the oxidative insertion step, the catalyst (PMe₃)Ni-alkyne interacts with the C(sp²)–H bond of the substrate. The difference in energetics arises presumably due to the changes in the formamide moiety as a result of AlMe₃ coordination. In the case of oxidative insertion transition state TS(**1a**-**2a**), the natural charge on nickel is found to be 0.02 more than that in TS(**1**–**2**), without AlMe₃. Since the process involves the conversion of Ni(0) to Ni(II), reduced population as noticed in TS(**1a**-**2a**), is more favorable. This lowering of population at the metal center is attributed to AlMe₃ coordination with the formyl group.¹⁶

(14) Optimized geometries of key transition states without AlMe₃ coordination are provided in Figure S3 in the Supporting Information.

(15) A Similar C–H activation wherein the hydrogen is relayed through the metal center is noticed earlier. See: Roy, D.; Sunoj, R. B. *Org. Bimol. Chem* **2008**, *8*, 1040.

After having established the structural and energetic details on the formation of dihydropyridinone through a sequence of formyl C(*sp*²)-H followed by benzyl methyl C(*sp*³)-H bond activations, we wished to understand a potentially alternative possibility wherein the order of C-H bond activation is reversed. Such a possibility, termed pathway 2, involves the activation of benzyl methyl C(*sp*³)-H first, as shown in Scheme 3.¹⁷

Scheme 3. Mechanism of Ni/AlMe₃ Cooperative Catalysis Involving Dual C-H Activation Beginning with Benzylic Methyl C(*sp*³)-H Activation (pathway 2)



The Gibbs free energies for pathway 2 are provided in Table 1. In general, all the transition states in this pathway are found to be of higher energy as compared to the equivalent transition states noted earlier in pathway 1. More readily obvious from these data is that the transition state for the benzylic methyl C(*sp*³)-H bond activation is much higher in energy than the corresponding benzylic methyl bond activation in pathway 1. Furthermore, the subsequent transition state for the formyl C(*sp*²)-H activation TS(2a'-3a') occurring after benzylic methyl activation is of higher energy as well. On the basis of such distinct kinetic features, it is highly likely that the mechanism of

(16) (a) See Table S1 in Supporting Information. (b) An additional favorable orbital interaction between the developing Ni-C bond and the AlMe₃ fragment is noticed in TS(1a'-2a'') which is obviously absent in TS(1-2) (Figure S1 in Supporting Information)

dehydrogenative cycloaddition begins with formyl C-H activation as opposed to benzylic methyl C-H activation.

Table 1. Computed Gibbs Free Energies (in kcal/mol) for Important Transition States Involved in Pathway 2

TS	with AlMe ₃	without AlMe ₃
(1a'-2a')	42.7	53.2
(2a'-3a')	41.0	46.8
(4a'-5a')	19.0	28.4
(6a'-P)	10.9	24.4

A comparative analysis of the preferred order of C-H activation, starting with the formyl C(*sp*²)-H bond in pathway 1 with that of benzylic methyl C(*sp*³)-H bond in pathway 2, indicates that in the former the effect of a Lewis acid is readily felt at the formyl C-H bond. The incoming electron-rich Ni(0) catalyst would find it more conducive to insertion to the formyl C-H bond than to the benzylic methyl C-H bond which is farther from AlMe₃.

In conclusion, we have shown, using the computed Gibbs free energies, that the origin of cooperativity offered by AlMe₃ in the Ni(0) catalyzed dehydrogenative cycloaddition between alkynes and formamides arises due to the significant stabilization of the vital transition states as compared to the noncooperative pathways. The rate-limiting oxidative insertion has been found to be 14 kcal/mol lower in energy with the Lewis acid coordination than in its absence. The modulation of electronic effects due to the closer geometric proximity of the coordinated Lewis acid to the formyl group renders the preferred order of dual C-H activation as formyl C(*sp*²)-H first followed by benzylic methyl C(*sp*³)-H.

Acknowledgment. Generous computing time from IIT Bombay computer center is gratefully acknowledged. M.A. acknowledges an INSPIRE fellowship from DST-New Delhi. R.B.S. acknowledges BRNS-Mumbai for funding.

Supporting Information Available. Computational methods, Cartesian coordinates of all key stationary points, total electronic energies are provided. This material is available free of charge via the Internet at <http://pubs.acs.org>.

(17) The intermediate 2a'' resulting from the oxidative insertion converts to 2a' through a rotation.

The authors declare no competing financial interest.